Supporting Information

Muthurajan et al. 10.1073/pnas.1405005111

SI Materials and Methods

Protein Purification and Fluorescent Labeling. Poly [ADP ribose] polymerase 1 (PARP-1), an N-terminal DNA and chromatin binding portion (*N*-parp), and a C-terminal catalytic domain (*C*-parp) were purified and fluorescently labeled as described (1–3). Yeast nucleosome assembly protein 1 (Nap1) and histones were purified, and fluorescently labeled nucleosomes were assembled as published (4, 5). The fluorescently labeled samples behave identical to their unlabeled counterparts in gel shifts.

Trinucleosome Assembly and Quality Control. Unlabeled and fluorescently labeled trinucleosomes were assembled on 561-bp non–linker-ended (NLE) and 621-bp linker-ended (LE) DNAs as described (6), and checked for complete saturation using EcoRI digestion, analytical ultracentrifugation, and atomic force microscopy (Fig. S1 *D–F*) as described by Winkler et al. (6) and Muthurajan et al. (7).

EMSAs. One microliter of 4 μM NLE trinucleosome (NLE-Tri) or LE trinucleosome (LE-Tri) was incubated with 0.5-, 1.0-, 1.5-, or 2.0-fold excess of *N*-parp, *C*-parp, PARP-1, or automodified (AM) PARP-1 at room temperature (RT) for 30 min in a buffer containing 50 mM Tris (pH 7.5), 150 mM NaCl, and 2 mM arginine. The samples were analyzed on a 1% agarose gel in Tris-acetate-EDTA buffer at RT and 50 V for 200 min. Gels were stained with ethidium bromide, followed by Imperial stain (Thermo Scientific).

Atomic Force Microscopy Imaging. LE-Tri and NLE-Tri and their complexes with PARP-1 assembled as above were diluted in 20 mM Tris (pH 7.5) to ∼1.5 ng/μL, placed on 3-aminopropyltriethoxysilane–modified mica, and imaged and processed as described by Muthurajan et al. (7). A snapshot of the height profiles is shown in Fig. S1 *D–F*. Note that the height profile of nucleosomes in the absence of PARP-1 is ∼1.5–2 nM, as previously published (7).

High-Throughput Interaction by Fluorescence Intensity FRET Assay. Affinity measurements were performed as described by Clark et al. (1). Stoichiometries were obtained through Job plots, applying the continuous variation method (8). The total sample concentration was either 40 nM (*N*-parp) or 100 nM (PARP-1). The first titration step contained only trinucleosomes, and subsequent steps contained 10 nM (or 2 nM for *N*-parp) increments of PARP-1, replacing trinucleosomes in the complex. The last titration step contained PARP-1 alone and no trinucleosome. The data points were FRET-corrected (2) and plotted in GraphPad Prism using a second-order polynomial (quadratic) equation fit, with the mole fraction of PARP-1 on the *x* axis and normalized FRET-corrected values on the *y* axis. The maximum value on the curve indicated by a straight line drawn to the *x* axis is the stoichiometric equivalency point. A PARP-1 fraction of 0.5 M translates into a stoichiometry of 1:1 for PARP-1/trinucleosome.

Immunoprecipitation. U2OS cells cultured to 60–70% confluency were treated with 1 mM hydrogen peroxide (1 h at RT) in the presence or absence of PJ34 hydrochloride hydrate (PJ34) or gallotannin (50 μM each, 1 h at RT). Cells were washed with RT PBS, harvested, and gently lysed in a buffer containing 50 mM Tris (pH 7.5), 0.5% Nonidet P-40, and 420 mM NaCl. Soluble lysates were normalized by total protein concentrations and used for immunoprecipitation with IgG or poly [ADP-ribose] (PAR) antibody overnight. Protein G Dyna beads (Life Technologies) were added for additional 1-h incubation and washed, and bound proteins were eluted by boiling in SDS sample buffer. Eluates were analyzed by SDS/PAGE and immunoblotting with the antibodies indicated in Fig. 2*D*.

Automodification of PARP-1 and PAR Purification. Fluorescently labeled or unlabeled PARP-1 (720–2,000 nM) was incubated in 50 mM Tris·HCl (pH 8), 100 mM NaCl, 1 mM $MgCl_2$, and 1 mM DTT with 60 nM nicked 30-bp (30Nick) DNA and 600 μM NAD^+ at RT for 5 min, 2 h, or overnight. Samples were analyzed on 8% (wt/vol) SDS/PAGE or a 4–12% (vol/vol) Criterion XT (Biorad) gel. Upon automodification, AM–PARP-1 runs as a higher molecular weight smear (Fig. S3*A*; lanes 8, 11, 13, and 16–18). The attachment of fluorophores to PARP-1 does not have an impact on its ability to auto-PARylate (Fig. S3*B*). The modification reaction was quenched by adding PJ34 (1 mM final volume).

Isolation of PAR Chains. At various time points of PARP-1 automodification, PAR was purified from AM–PARP-1 as described (9). Commercially available PAR was obtained from Trevigen.

Nucleosome Disassembly Assay. One microliter of 3.3 μM-labeled nucleosome reconstituted onto "601" 165-bp DNA [Nuc165; cyanine 5 on H2B histone and Alexa488 on H4 histone] was incubated with a 1.5-fold molar excess of unlabeled PARP-1 at RT for 30 min in a buffer containing 25 mM Tris (pH 7.5), 150 mM NaCl, and 1.5 mM $MgCl_2$. The reaction was spiked with 60 nM 30Nick DNA to ensure enzymatic activation of PARP-1. Ten microliters of this master mix was incubated with increasing amounts of NAD^+ (final concentrations of 0.1, 1, 10, 20, and 40 μM) in a final volume of 20 μL at RT for 30 min (10). The samples were loaded onto a prerun 5% (wt/vol) native PAGE gel run at 150 V and 4 °C for 1 h. The gel was scanned on a Typhoon Trio (GE Healthcare) variable mode imager, at acceptor (633/670), donor (488/520), and FRET (488/670) wavelengths. Duplicates of the reactions were analyzed on a 4–12% (wt/vol) Criterion XT gel to monitor the extent of automodification of PARP-1 and histones by Imperial staining and anti-PAR Western blot.

H2A-H2B Removal Assay. Ten nanomolar Nuc165 was incubated with 70 nM refolded H2A–H2B dimer at RT for 30 min. The reaction was further incubated at RT for 1 h with increasing amounts of unmodified or AM–PARP-1 as indicated. The samples were run on a 5% (wt/vol) native polyacrylamide gel in 0.2× Tris-borate-EDTA (TBE) at 150 V for 1 h at 4 °C and then stained with SyBr Gold (Invitrogen).

Rescue of Aggregated Chromatin Assay. Ten nanomolar 165-bp DNA was incubated with 10 nM Alexa488-labeled H3–H4 complex and 120 nM Atto647N-labeled H2A–H2B complex complete in 25 mM Tris (pH 7.5), 200 mM NaCl, 0.01% Nonidet P-40, and 0.01% CHAPS. Aliquots of this mixture were incubated with increasing amounts (10, 50, and 120 nM) of AM–PARP-1, *N*-parp, *C*-parp, a mock automodification reaction, or PARP-1. Nucleosome assembly reactions were analyzed on 5% native PAGE in 0.2× TBE at 300 V and 4 °C for 2 h. The gel was scanned on a Typhoon Trio variable mode imager as described above. The nucleosomes assembled in this assay were subjected to micrococcal nuclease digestion to verify the length of DNA protected (11). The histone content of these nucleosomes was analyzed by excising the nucleosome band from the native gel,

eluting it, and running it on a 4–12% (wt/vol) Criterion XT gel (12). The gel was scanned as described above before staining it with silver stain.

DNA Supercoiling Assay. The assay was performed as published (13), with the difference that pGEM-3Z vector (Promega) was used to assemble nucleosomes.

1. Clark NJ, Kramer M, Muthurajan UM, Luger K (2012) Alternative modes of binding of poly(ADP-ribose) polymerase 1 to free DNA and nucleosomes. *J Biol Chem* 287(39): 32430–32439.
2. Hieb AR, D'Arcy S, Kramer MA, White AE, Luger K (2012) Fluorescence strategies for high-throughput quantification of protein interactions. *Nucleic Acids Res* 40(5):e33.
3. Winkler DD, Luger K, Hieb AR (2012) Quantifying chromatin-associated interactions: The HI-FI system. *Methods Enzymol* 512:243–274.
4. Andrews AJ, Downing G, Brown K, Park YJ, Luger K (2008) A thermodynamic model for Nap1-histone interactions. *J Biol Chem* 283(47):32412–32418.
5. Dyer PN, et al. (2004) Reconstitution of nucleosome core particles from recombinant histones and DNA. *Methods Enzymol* 375:23–44.
6. Winkler DD, Muthurajan UM, Hieb AR, Luger K (2011) Histone chaperone FACT coordinates nucleosome interaction through multiple synergistic binding events. *J Biol Chem* 286(48):41883–41892.
7. Muthurajan UM, McBryant SJ, Lu X, Hansen JC, Luger K (2011) The linker region of macroH2A promotes self-association of nucleosomal arrays. *J Biol Chem* 286(27): 23852–23864.
8. Olson EJ, Bühlmann P (2011) Getting more out of a Job plot: determination of reactant to product stoichiometry in cases of displacement reactions and n:n complex formation. *J Org Chem* 76(20):8406–8412.
9. Panzeter PL, Zweifel B, Althaus FR (1994) Fast protein liquid chromatographic purification of poly(ADP-ribose) polymerase and separation of ADP-ribose polymers. *J Chromatogr A* 678(1):35–40.
10. D'Amours D, Desnoyers S, D'Silva I, Poirier GG (1999) Poly(ADP-ribosyl)ation reactions in the regulation of nuclear functions. *Biochem J* 342(Pt 2):249–268.
11. Chen CC, et al. (2014) CAL1 is the Drosophila CENP-A assembly factor. *J Cell Biol* 204(3):313–329.
12. Dechassa ML, Wyns K, Luger K (2014) Scm3 deposits a (Cse4-H4)2 tetramer onto DNA through a Cse4-H4 dimer intermediate. *Nucleic Acids Res* 42(9):5532–5542.
13. Dechassa ML, et al. (2011) Structure and Scm3-mediated assembly of budding yeast centromeric nucleosomes. *Nat Commun* 2:313.

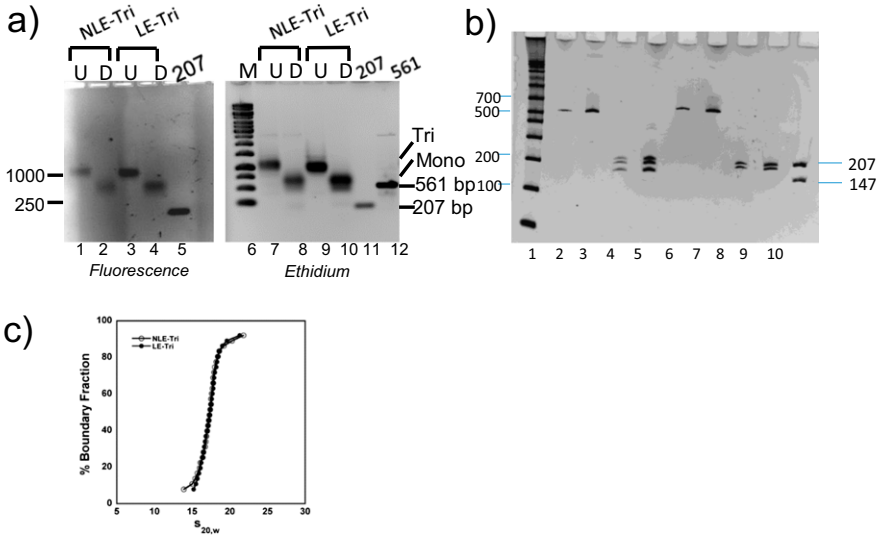

Fig. S1. (Continued)

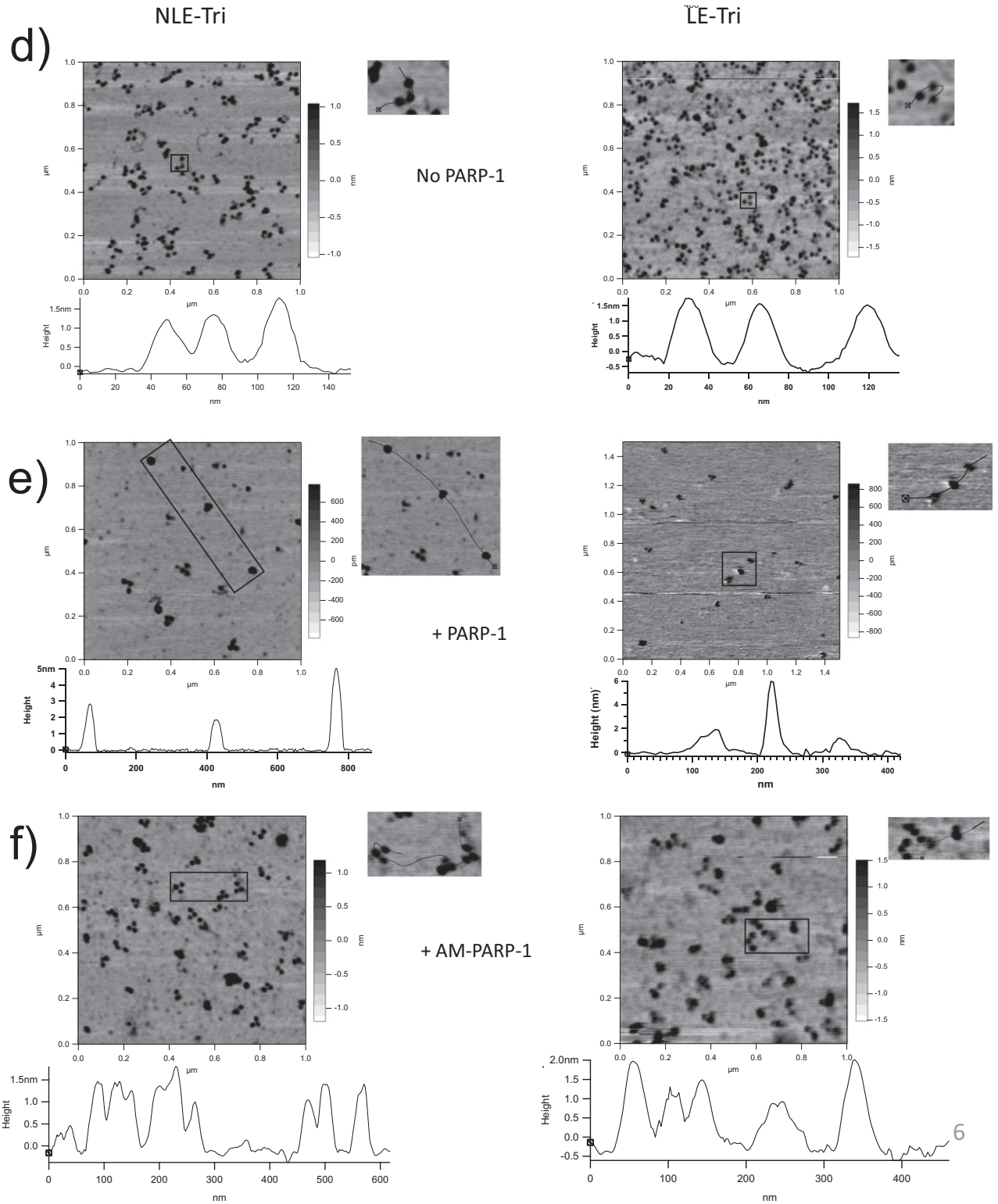

Fig. S1. Quality control of trinucleosomes and PARP-1 binding. (*A*) EcoRI digestion assay. Atto647N-labeled NLE and LE trinucleosomal arrays were digested into mononucleosomes (lanes designated with D) and run on an agarose gel in Tris acetate–EDTA buffer at 50 V for 2 h, alongside uncut controls (lanes designated with U). No 207-bp free DNA is observed in the digested lanes, demonstrating that all three positioning sites are occupied by nucleosomes in the arrays. Lanes 1 and 7 contain undigested NLE-Tri, lanes 2 and 8 contain digested NLE-Tri, lanes 3 and 9 contain undigested LE-Tri, lanes 4 and 10 contain digested LE-Tri, lanes 5 and 11 contain 207-bp DNA, and lane 6 contains a DNA size marker (M). Lane 12 contains 561-bp NLE DNA. (*B*) Five micrograms each of NLE-Tri and LE-Tri were either digested with 5 µL of EcoRI or mock-treated. The samples were phenol-chloroform-isoamyl alcohol–extracted and ethanol-precipitated, and pellets were dissolved in nuclease-free water. The samples were run on a 10% native TBE gel and stained with ethidium bromide. Lane 1 contains ladder, lanes 2–3 contain undigested NLE DNA (10 and 50 ng, respectively), lanes 4–5 contain EcoRI-digested NLE DNA (10 and 50 ng, respectively),

Legend continued on following page

lanes 6–7 contain undigested LE DNA (10 and 50 ng, respectively), lanes 8–9 contain EcoRI-digested LE DNA (10 and 50 ng, respectively), and lane 10 contains a mixture of 207-bp and 147-bp DNAs. For NLE DNA, the EcoRI-digested fragments are 161, 207, and 193 bp, and for LE DNA, the fragment sizes are 207 and 161 bp, indicating that the latter has extended linker arms on the outer nucleosomes. (*C*) Sedimentation velocity analysis ultracentrifugation profile for Atto647N-labeled trinucleosomes with a midpoint of ~17S–18S, indicating complete saturation of the nucleosomal arrays. (*D–F*) Atomic force microscopy of trinucleosomes and trinucleosome–PARP-1 complexes. Scans (1–1.5 μm) are shown. Trinucleosomes (*D*) with PARP-1 (*E*) and with AM–PARP-1 (*F*) are shown. Height profiles of selected particles are shown underneath each panel.

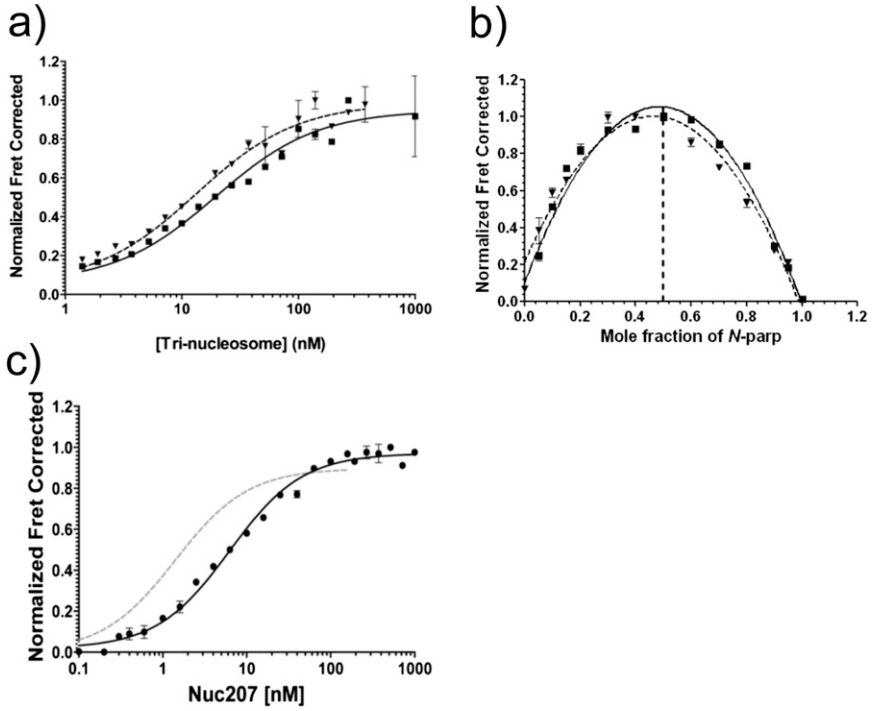

Fig. S2. Determination of binding constants and stoichiometries for *N*-parp. (*A*) Representative binding curves of *N*-parp to NLE-Tri (dashed line; solid symbols) and LE-Tri (solid line; solid symbols); K_d values are listed in Table 1. (*B*) Stoichiometry of the *N*-parp–trinucleosome complex, determined by a Job plot. (*C*) Representative binding curves of Nuc207 with unmodified PARP-1 (dashed line, as in figure 4C in ref. 1) and AM–PARP-1 (solid line).

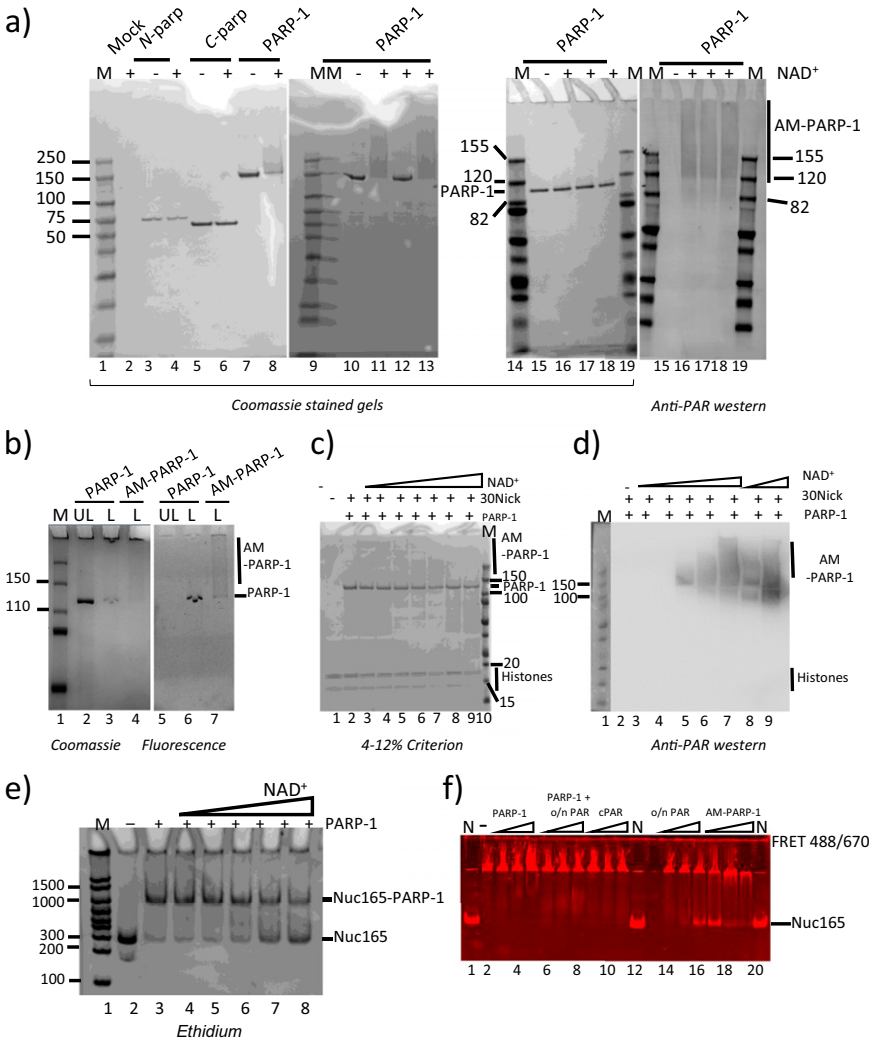

Fig. S3. PARP-1 undergoes automodification, whereas *N*-parp and *C*-parp do not. Automodification reactions for *N*-parp, *C*-parp, and PARP-1 were set up as described in *SI Materials and Methods*. (*A*) SDS/PAGE of AM–PARP-1 constructs. Lane 1 contains marker, lane 2 contains "mock" (no PARP-1), lanes 3–4 contain *N*-parp, lanes 5–6 contain *C*-parp, lanes 7–8 contain PARP-1, lane 9 contains size markers (MM), lanes 10–11 contain PARP-1, lane 12 contains PARP-1 inhibitor PJ34 added before NAD^+, lane 13 contains PJ34 after overnight incubation with NAD^+, lanes 14 and 19 contain ladder, lane 15 contains PARP-1, lane 16 contains AM–PARP-1 after a 5-min incubation, lane 17 represents a 2-h incubation, and lane 18 represents overnight incubation. (*Right*) Western blot probed with anti-PAR antibodies shows similar levels of automodification for 5-min, 2-h, and overnight modified samples. (*B*) Fluorescently labeled PARP-1 can be modified. Lane 1 contains a size marker, lane 2 contains unlabeled (UL) PARP-1, lanes 3 and 6 contain Alexa488-labeled (L) PARP-1, and lanes 4 and 7, contain Alexa488-labeled (L) AM–PARP-1. (*C*) Samples used in Fig. 2*E* were analyzed on a 4–12% Criterion XT gel to check the extent of PARP-1 automodification, as well as to look for histone heteromodification. Lane 1 contains Nuc165; lane 2 contains Nuc165 + 1.5-fold excess PARP-1 + 30mer DNA; lanes 3–7 contain the complex in lane 2 with 0.1, 1, 10, 20, and 40 μM NAD^+; lanes 8–9 contain samples as in lanes 6–7, respectively, but incubated overnight; and lane 10 contains markers. (*D*) Western blot analysis of samples in *C*. Increasing PARylation is evident with increasing concentrations of NAD^+, and there is a greater PAR signal for overnight-incubated samples. Lane 1 shows markers; lane 2 contains Nuc165 + 1.5-fold excess PARP-1 + 30mer DNA; lanes 3–7 contain Nuc165 with 1.5-fold excess PARP-1, with 0.1, 1, 10, 20, and 40 μM NAD^+; and lanes 8–9 contain samples as in lanes 6–7, respectively, but incubated overnight. No PARylation of histones was observed. Lane 1 was visualized by white light, whereas the rest of the blot was developed by chemiluminescence and visualized by UV imaging. (*E*) Same gel as in Fig. 2*E* stained with ethidium bromide to confirm that no free DNA is released upon addition of NAD^+. Lane 2 contains nucleosomes alone; lane 3 contains nucleosomes with PARP-1 and 30Nick DNA; and lanes 4–8 contain the complex in lane 3 and 0.1, 1, 10, 20, and 40 μM NAD^+, respectively. (*F*) PAR bound to PARP-1 is more efficient in the rescue of aggregated chromatin assay than PAR chains cleaved off of AM–PARP-1. The experiment was performed as described for Fig. 3 *D*–*F*. Lanes 1 and 12 contain nucleosome (N); lane 2 contains DNA and histones as in Fig. 3*D*; lanes 3–5 contain 10, 50, and 120 nM PARP-1; lanes 6–8 contain 10, 50, and 120 nM PARP-1 and the same amount of PAR purified from overnight AM–PARP-1; lanes 9–11 contain 10, 50, and 120 nM commercially available (cPAR); lane 13 is empty; lanes 14–16 contain 10, 50, and 120 nM PAR from overnight AM–PARP-1; and lanes 18–20 contain 10, 50, and 120 nM AM–PARP-1.

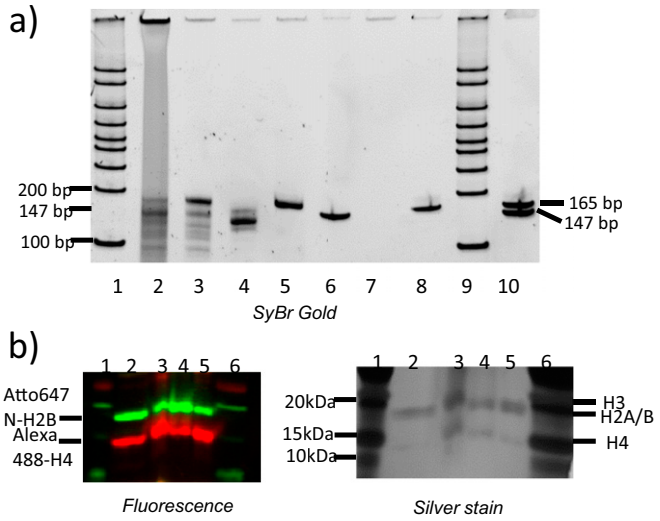

Fig. S4. Quality control of nucleosomes assembled via rescue of aggregated chromatin assay. (*A*) Nucleosomes assembled in the assay shown in Fig. 3*D* were digested with micrococcal nuclease (MNase) and run on a 5% native TBE gel. Yeast NAP1 (yNap1)- and AM–PARP-1–assembled nucleosomes show similar protection of 165-bp DNA upon MNase digestion. Lanes 1 and 9 contain markers, lane 2 contains AM–PARP-1–assembled nucleosomes (the smear observed in this lane is due to the presence of PAR), lane 3 contains yNap1-assembled nucleosomes, lane 4 contains salt dialysis-reconstituted nucleosomes, lane 5 contains undigested 165-bp DNA, lane 6 contains 147-bp DNA, lane 7 contains MNase-digested 165-bp DNA, lane 8 contains 165-bp DNA, and lane 10 contains 165-bp + 147-bp DNA. (*B*) Histone content of nucleosomes assembled in the RAC assay. Nucleosome bands were excised from a 5% native gel and run on SDS/PAGE. (*Left*) Fluorescence scan overlay of Atto647N-labeled H2B and Alexa488-labeled H4 histones. The gel was subsequently silver-stained, and all four histone bands were visualized, confirming that AM–PARP-1 was capable of assembling bona fide nucleosomes. Lanes 1 and 6 contain size markers, lane 2 contains doubly labeled histone octamer, lane 3 contains AM-Parp1–assembled nucleosome, lane 4 contains Nap1-assembled nucleosomes, and lane 5 contains nucleosomes assembled by salt dialysis.